Polarization and Velocity Dependence of Associative Ionization in Na(3p)+Na(3p) Collisions

Meijer, Harro; Meulen, H.P. van der; Morgenstern, R.

Published in:
Zeitschrift f%EF%BF%BDr Physik D Atoms%2C Molecules and Clusters

DOI:
10.1007/BF01385460

Publication date:
1987

Z. Phys. D – Atoms, Molecules and Clusters 5, 299–308 (1987)

Atoms, Molecules
Zeitschrift für Physik D and Clusters

Polarization and Velocity Dependence of Associative Ionization in Na($3p$) + Na($3p$) Collisions

H.A.J. Meijer, H.P. van der Meulen, and R. Morgenstern
Fysisch Laboratorium, Rijksuniversiteit Utrecht, Utrecht, The Netherlands

Received March 13, 1986; final version December 18, 1986

We have excited Na atoms of two counterrunning thermal beams by means of linearly polarized laser light and have investigated associative ionization processes. To this end we measured the total ionization signal as a function of the angle θ between light polarization and the relative collision velocity. Velocities of the excited atoms were selected by exploiting the Doppler effect. We found an increasing polarization dependence at increasing collision velocities. At all velocities the preparation of the collision partners in the $|M_j|=1/2$ sublevel of the Na $^2P_{3/2}$ state is most efficient in producing ionization.

PACS: 34.30.th; 34.50.Fa; 34.50.Rk

1. Introduction

Associative ionization of excited atoms is an important ionization process in gases that are exposed to resonance radiation which can excite the atoms in the gas, but cannot ionize them in a one-step photoionization process. Associative ionization of excited Na atoms according to the reaction

$$\mathrm{Na}(3p)\,^2P_{3/2} + \mathrm{Na}(3p)\,^2P_{3/2} \rightarrow \mathrm{Na}_2^+ + e^- \qquad (1)$$

is a process which has been investigated by various groups in the past. In the first experiments ions [1–5] or electrons [6] from process (1) were observed without paying too much attention to the exact state preparation of the excited collision partners before the collision, especially their polarization. However, the collision system of two excited Na atoms is ideally suited for a more detailed investigation, since an exact preparation of the collision partners with respect to their polarization and also their relative velocity before the collision is possible. The dependence of process (1) on the polarization of the collision partners has been investigated more recently by various groups and all experiments yield roughly the same results [7–10]. However there were indications [9] that the polarization dependence of process (1) varies when the collision velocity varies from subthermal to thermal velocities. We therefore started a systematic study of this velocity dependence. Recently Wang et al. [11] reported on the velocity dependence of process (1). However in that experiment only circularly polarized light was used for the excitation of the atoms whereas we use linearly polarized light. By this we can vary the atomic polarization for each collision velocity. In this respect our new experiment is more detailed than that of Wang et al. [11].

2. Experiment

The experimental setup is shown schematically in Fig. 1. Two thermal beams of Na atoms effusing from ovens in opposite directions intersect each other. They are collimated to a height of 10 mm and a width of 0.5 mm. They are intersected at nearly right angles by laser light from a CW-ring-dyelaser (Spectra Physics 380D), tuned to the $F=2 \rightarrow F'=3$ hyperfine component of the $\mathrm{Na}(3s)\,^2S_{1/2} \rightarrow \mathrm{Na}(3p)\,^2P_{3/2}$ transition. The laser beam is expanded and directed through a rectangular diafragm, resulting in a spatially homogeneous laser spot with a height of 9 mm and a width of 5 mm. The angular divergence of the Na beams in the direction of the laser light is only 4 mrad. The

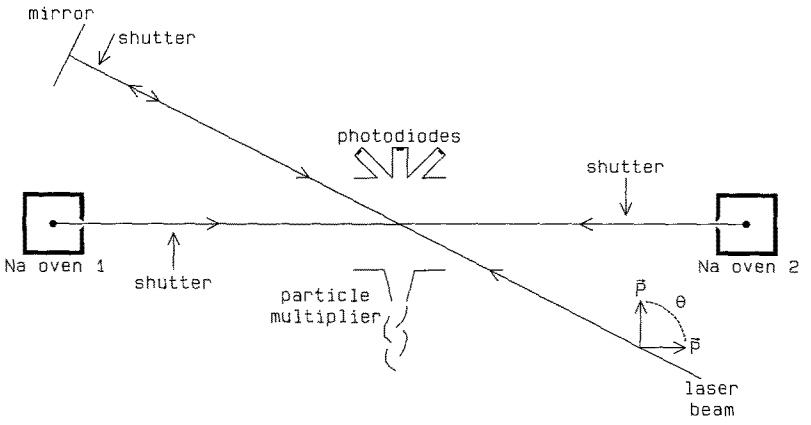

Fig. 1. Schematic view of the experimental setup. For explanation see text

rectangular laser spot defines the interaction region, where ions can be formed according to process (1). The atomic densities in this interaction region are estimated to be $4 \cdot 10^9$ and $6 \cdot 10^9/\text{cm}^3$ for the two beams, respectively. All ions created in the interaction region are extracted by a small electric field (100 V/cm) and are counted by a particle multiplier. The fluorescence light is monitored by photodiodes. Thereby we are able to keep track of the excited atom density and the atomic polarization. The ion production rate is measured for different collision velocities as a function of the angle θ between the linear polarization vector of the laser light and the direction of the atomic beams. This angle θ is varied by rotating the polarization vector by means of a double Fresnel rhomb (Spectra Physics 310), in combination with a rotatable polaroid. The ionization signal I contains (besides a small background signal I_B) components I_{12}, I_{11}, I_{22} which are respectively due to collisions of excited atoms from different atomic beams, of excited atoms within beam 1 or within beam 2. To separate these signals we use beamshutters for the laser and the atomic beams, which are opened and closed in various combinations. Each signal is measured several times for one second and it is checked that all measurements yield the same result within the statistical error. The whole data acquisition procedure is performed with an Apple II computer, which controls the beamshutters, checks the laser frequency and the laser intensity, directs the polarization rotator for the laser light and reads and checks the signals from the particle multiplier as well as from the photodiodes.

2.1. *Velocity Selection of Excited Atoms and Calculations of Cross Sections*

In order to excite only atoms with well-defined velocity by the laser light we exploit the Doppler effect. For this we direct the laser light to the atomic beams such that laser beam and atomic beam 2 form an angle of $\alpha = 87°$. Then laser light with a frequency ν_L is "seen" by an atom of beam 2 having velocity v_2 as:

$$\nu_L' = \nu_L\left(1 - \frac{v_2}{c}\cos\alpha\right), \tag{2}$$

with c the speed of light.

For this atom the laser has an effective spectral volume density $\rho_{\nu_{\text{eff}}}$ of:

$$\rho_{\nu_{\text{eff}}} = \int \mathrm{d}\nu'\, I_L(\nu', \nu_L')\, S(\nu', \nu_0), \tag{3}$$

with $I_L(\nu', \nu_L')$ the laser intensity at frequency ν', while the maximum of the frequency distribution is at ν_L', and $S(\nu', \nu_0)$ the absorption profile of the atomic transition, with the maximum at ν_0. If the bandwidth of the laser is much smaller than the natural linewidth of the atomic transition $\Delta\nu_0$, we get:

$$\rho_{\nu_{\text{eff}}} = \frac{\rho_\nu}{1 + 4\left(\dfrac{\nu_L' - \nu_0}{\Delta\nu_0}\right)^2} \tag{4}$$

Together with the general expression for the relative population n_e of the excited level:

$$\frac{n_e}{n_0} = \tfrac{1}{2}[1 + \rho_s/\rho_{\nu_{\text{eff}}}]^{-1} \tag{5}$$

(with n_0 the total number of atoms interacting with the laser, and ρ_s the saturation parameter we get, after some straightforward calculations:

$$\frac{n_e}{n_0} = \tfrac{1}{2}[1 + \rho_s/\rho_\nu]^{-1}\left[1 + 4\left(\frac{\nu_L' - \nu_0}{\Delta\nu_s}\right)^2\right]^{-1}. \tag{6}$$

The functional dependence of the fraction of excited atoms on the laser detuning thus turns out to have a Lorentz profile with a saturation broadened width $\Delta\nu_s$ given by:

$$\Delta\nu_s=\Delta\nu_0\left(1+\frac{\rho_\nu}{\rho_s}\right)^{1/2} \tag{7}$$

The saturation parameter ρ_s is dependent on the polarization of the exciting laserbeam. In our case (with linearly polarized light), and by using:

$$\int I_L(\nu)\,\mathrm{d}\nu\equiv\frac{E}{c}, \tag{8}$$

with E the laser irradiance, we get

$$\Delta\nu_s=[95+8.3E]^{1/2} \tag{9}$$

($\Delta\nu_0=9.8$ MHz, E in mW/cm^2), but in case we use circularly polarized light [12], we get:

$$\Delta\nu_s=[95+15.3E]^{1/2}. \tag{10}$$

From (6) we see that, at a certain spectral volume density of the laser, the probability of being in an excited state depends on the detuning $(\nu_L'-\nu_0)$ and differs from resonant tuning by a factor $A(\nu_L')$, given by:

$$A(\nu_L')=\left(1+4\left(\frac{\nu_L'-\nu_0}{\Delta\nu_s}\right)^2\right)^{-1} \tag{11}$$

Combining (2) and (11) we get the velocity-dependent (relative) probability of being in an excited state:

$$A(\nu_L,\nu_2)=\left\{1+4\left(\frac{\nu_0-\nu_L+\nu_L\left(\frac{\nu_2}{c}\right)\cos\alpha}{\Delta\nu_s}\right)^2\right\}^{-1}. \tag{12}$$

Resonance occurs for $\nu_L>\nu_0$. By tuning the laser we can select the velocity-distribution of the excited atoms. Because of the opposite velocity of the atoms in beam 1, they will not be excited simultaneously with the atoms in beam 2. In order to get also excited atoms in beam 1 – and thus allow for "head-head" collisions of excited atoms from different beams – we reflect the laser beam in itself with a mirror behind the interaction region. The reflected laser beam intersects atomic beam 1 at 87°, and thus excites atoms in atomic beam 1 according to (12).

Because of the Maxwell-Boltzmann velocity distribution $M(\nu_i, T_i)$ (T_i oven temperature) in our atomic beams the velocity distribution of excited atoms is:

$$g_i(\nu_i,\nu_L)=A(\nu_L,\nu_i)\,M(\nu_i,T_i) \tag{13}$$

The number N_i of excited atoms per unit volume in beam i (and therefore the total fluorescence I_f) is proportional to the integral of (13) over all velocities ν_i. The velocity distribution of the atomic beams has been checked by measuring I_{f_1} and I_{f_2} as a function of ν_L. The results were in very good agreement with

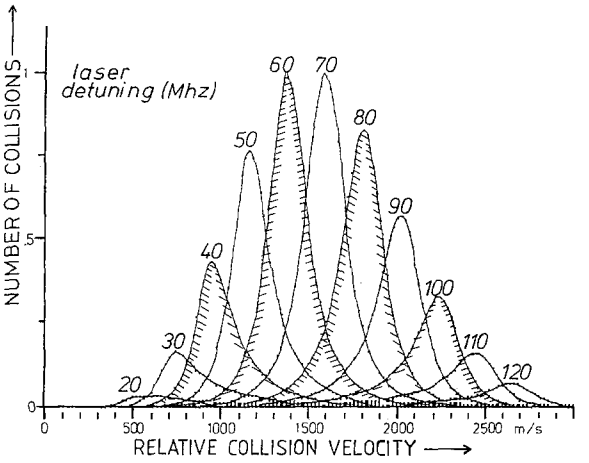

Fig. 2. Number of collisions as a function of the relative collision velocity v_c vs. v_c, at different laser detunings. It shows the velocity resolution, as achieved in our experiments

the numerical calculations, using (13). The number of collisions N_c (per unit of interaction volume, unit of time and unit of cross section) between excited atoms from beam 1 and beam 2 becomes:

$$N_c(\nu_L)=\int_{\nu_1}\int_{\nu_2}\mathrm{d}\nu_1\,\mathrm{d}\nu_2\,g_1(\nu_1,\nu_L)\,g_2(\nu_2,\nu_L)(\nu_1+\nu_2). \tag{14}$$

This expression can also be written:

$$N_c(\nu_L)=\int_{\nu_c}\nu_c\left[\int_{\nu_1}g_1(\nu_1,\nu_L)\,g_2(\nu_c-\nu_1,\nu_L)\,\mathrm{d}\nu_1\right]\mathrm{d}\nu_c, \tag{15}$$

with v_c the relative collision velocity. The integrand $n_c(\nu_c,\nu_L)\equiv\nu_c\int_{\nu_1}g_1(\nu_1,\nu_L)\,g_2(\nu_c-\nu_1,\nu_L)\,\mathrm{d}\nu_1$ represents the number of collisions with relative collision velocity v_c. In Fig. 2 we show several distributions n_c for different laser frequencies ν_L which differ from the resonance frequency ν_0 of an atom at rest by values between 20 and 120 MHz. For these calculations we assumed oven temperatures of 635 and 575 K respectively, and $E=8$ mW/cm^2, resulting in $\Delta\nu_s=13$ MHz. One can see that for laser detunings far from the maximum at ~65 MHz we obtain strongly asymmetric distributions n_c. Furthermore note that the area under the curves equals N_c, which of course varies strongly with the laser frequency. The average collision velocity $\bar{v}_c$ is:

$$\bar{v}_c(\nu_L)=\frac{\int_{\nu_c}\nu_c\cdot n_c\,\mathrm{d}\nu_c}{N_c} \tag{16}$$

The total number of ions produced is proportional to:

$$R=\int_{\nu_c}n_c(\nu_c,\nu_L)\,\sigma(\nu_c)\,\mathrm{d}\nu_c, \tag{17}$$

with $\sigma(v_c)$ the velocity dependent cross section for process (1), apparently also depending on the polarization of the colliding atoms (see 2.2). Finally, the cross section $\sigma(\bar{v}_c)$, averaged over the velocity distribution n_c, becomes

$$\sigma(\bar{v}_c)=\frac{R}{N_c}. \tag{18}$$

In the experiment, we can measure the ion signal R, but not N_c. However, it is easy to calculate, by numerical integration,

$$v_{\text{eff}}\equiv\frac{N_c}{N_1 N_2}, \tag{19}$$

with N_i the density of excited atoms in beam i.

This v_{eff} is also a velocity average over n_c, like $\bar{v}_c$, but with a different weight factor. It appears to be slightly smaller than $\bar{v}_c$. We can measure the fluorescence signals I_{f_1} and I_{f_2}, which are proportional to N_1 and N_2. Furthermore we know the temperatures of the ovens, the laser frequency ν_L, as well as the laser irradiance E, and the angle α. Then:

$$\sigma(\bar{v}_c)=\frac{R}{N_c}\propto\frac{R}{I_{f_1}I_{f_2}v_{\text{eff}}}. \tag{20}$$

It should be pointed out that collisions at very low relative velocity occur between atoms within one atomic beam. For these "head-tail" collisions v_{eff} and $\bar{v}_c$ can also be calculated using (19) and (16), if one keeps in mind that both colliding atoms are in the same atomic beam, therefore having the same velocity direction. Both v_{eff} and $\bar{v}_c$ show hardly any variation with ν_L, but, since the collision velocity distributions in head-tail collisions are very broad, v_{eff} differs much more from $\bar{v}_c$ than in the head-head case.

The method of velocity selection by Doppler-tuning asks for an especially good laser stabilization. Commercial stabilization systems operating with temperature-stabilized Fabry-Pérot etalons normally allow a long time frequency drift of $\sim$40 MHz/h. As can be seen from Fig. 2 this is not acceptable for our experiment. We therefore have developed our own stabilization system which couples the laser frequency to atomic fluorescence signals and which allows to stabilize the laser to within 1 MHz in a range of $\pm$120 MHz from the resonance frequency ν_0 [12].

2.2. Atomic Polarization

For sufficiently high laser intensity a stationary population of the magnetic sublevels of the $F'=3$ state is obtained. In a coordinate frame with z parallel to the light polarization vector the excited atoms are described by a diagonal density matrix with elements in ratios of 20:10:10:0 for $M_F=0$, ±1, ±2 and ±3 respectively [13,14]. From this one can deduce a density matrix for only the electronic part of the wavefunction by taking the trace over nuclear spin components M_I. The elements of the resulting diagonal matrix ($\rho_{1/2}$ and $\rho_{3/2}$) have ratios of 5:1 for $M_j=\pm1/2$ and $\pm3/2$ respectively (J is the electronic angular momentum). This matrix can further be reduced if only orbital angular momentum is important. Taking the trace over electronic spin components M_s one arrives again at a diagonal matrix with elements (ρ_0 and ρ_1) in a ratio of 2:5:2 for $M_L=-1$, 0, 1 respectively.

In order to check if this stationary state is obtained we have always measured the resonance fluorescence signal at the photodiodes as a function of the angle β between the directions of the laser polarization vector and photodiodes. This fluorescence intensity can be described by:

$$I_f=I_0(1+B\sin^2\beta), \tag{21}$$

with $B=0.75$ following from the ratio 5:2 for the M_L sublevels.

2.3. Laser Intensity Considerations

To obtain the stationary state described in the preceding section one has to allow for a sufficiently large number of excitation and decay cycles for each atom on its way through the laser spot. For this a sufficiently high laser intensity is needed. On the other hand the laser intensity has to be chosen sufficiently low in order to avoid "trapping" effects: one has to avoid as much as possible excitation of the $F'=2$ hyperfine level (59 MHz below the $F'=3$ level) which decays to the "wrong" hyperfine level $F=1$ of the ground state with a probability of 1/2. From this level, which lies 1700 MHz below the $F=2$ ground level, atoms are not excited by the laser anymore. Such a "trapping" leads to an exponential decrease of excited atoms along the way of the atomic beam through the laser spot. For our case of two counterpropagating atomic beams this can influence the experimental results considerably: relatively few collisions between excited atoms from different beams occur although a high overall density of excited atoms is indicated by the fluorescence signal at the photodiodes. This simulates a too low ionization cross section, especially at low atomic velocities where the trapping becomes increasingly important.

To get an idea which laser intensity is appropriate for our experiments we have numerically calculated the population of the excited $F'=3$ state and its suble-

vels and the resulting β-dependent fluorescence intensity as a function of the laser irradiance, with a mean passage time of 6 μs. We have done this for excitation with linearly (π) as well as circularly (σ) polarized light. In the circular case trapping effects caused by the $F'=2$ state play a minor role [15]. These numerical calculations show that in the σ-case the steady state assumption is no longer valid at laser irradiances below 3 mW/cm^2 (in the π-case 0.5 mW/cm^2), i.e. there is a considerable change of atomic polarization throughout the laser spot.

The results of our calculations are in good agreement with measurements of fluorescence intensities as a function of laser irradiance, that we performed[1]. Out of this comparison we conclude that we have to use laser irradiances higher than 3 mW/cm^2 (for steady state), and lower than 15 mW/cm^2 (to avoid trapping in the π-case). Our experiments have in fact been performed with irradiances of 8 mW/cm^2.

2.4. Influence of the Velocity Selection Method on Atomic Polarization

In our experiments B (21) showed a systematic variation: for excitation of atoms with low velocity we found $B=0.6$, for high velocities we found 0.85. The explanation of this systematic variation lies in the fact that for excitation of atoms with low velocity comparatively many atoms "see" the laser light with a frequency lower than the resonance frequency ν_0, whereas high velocity selection causes many atoms to see the laser frequency higher than ν_0. In both cases the $F=2\rightarrow F'=2$ transition becomes relatively more important. It is the interference of the $F=2\rightarrow F'=2$ and $F=2\rightarrow F'=3$ transitions that causes the systematic changes in B. This means that the steady state ratio 5:1 for $\rho_{1/2}$ and $\rho_{3/2}$ is in general not achieved in our experiments. Therefore, instead of this ratio, we used the experimental ratio, based on the measurements of B. One can derive: $\rho_{1/2}/\rho_{3/2}=(3+6B)/(3-2B)$. The ionization signal can conveniently be expressed in terms of the ratio Q given by:

$$Q\equiv\frac{\rho_{3/2}+\rho_{1/2}}{\rho_{3/2}-\rho_{1/2}}=-\frac{3+2B}{4B}. \tag{22}$$

The other complication is that the fluorescence intensity now has a varying angular distribution. Therefore the fluorescence signal, as detected at $\beta=90°$, no longer represents a constant ratio of the total fluorescence and thus of the total population. We solved this problem by detecting the fluorescence at $\beta=54.7°$, the "magic angle", at which transitions from both the $M_L=\pm1$ and $M_L=0$ upper levels yield the same amount of light.

[1] These calculations and measurements are discussed in more detail by Alkemade [16]

3. Theory

As was discussed by Kircz et al. [7] the most detailed quantities describing the associative ionization of the two atoms are the amplitudes $f(\alpha\mathbf{v}_f\leftarrow M_1M_2\mathbf{v}_c)$, with M_1, M_2 the initial magnetic quantum numbers of the excited atoms, $\mathbf{v}_c$ the collision velocity, $\mathbf{v}_f$ the velocity of the ejected electron and α representing the state of the resulting molecular ion.

Absolute square values of these amplitudes f represent ionization cross sections $\sigma(\alpha\mathbf{v}_f\leftarrow M_1M_2\mathbf{v}_c)$. The observed ion production rate can be expressed by:

$$\begin{aligned}R=N_c\int\mathrm{d}\Omega_f\int\mathrm{d}v_f\sum_{\alpha M_1M_2M_1'M_2'}&[f(\alpha\mathbf{v}_f\leftarrow M_1M_2\mathbf{v}_c)\\&\cdot f^*(\alpha\mathbf{v}_f\leftarrow M_1'M_2'\mathbf{v}_c)(mv_f/\mu)]_{av}\\&\cdot\langle M_1|\rho|M_1'\rangle\langle M_2|\rho|M_2'\rangle.\end{aligned} \tag{23}$$

Here we have integrated and summed over the unobserved properties of the final state. The part between square brackets has to be averaged over the remaining velocity distribution of $\mathbf{v}_c\cdot N_c$ is the number of collisions (14) and μ is the reduced mass of the resulting molecular ion. The normalized density matrix elements $\langle M|\rho|M'\rangle$ for the excited atoms are obtained by rotating the diagonal density matrix (which is known by measuring B and applying (22)) from the "light frame" (with z parallel to the light polarization vector) by an angle θ to the "collision frame" (with z parallel to $\mathbf{v}_c$). This is done by means of a rotation matrix $D(0,\theta,0)$ [17]. We assume that the ionization process is not influenced by nuclear spin orientation and therefore start from the density matrix for M_j with $J=3/2$, which is rotated to the collision frame by a rotation matrix $D^{3/2}(0,\theta,0)$. Nienhuis [18] has shown in more detail that in this case the θ-dependence of the ion production rate R can be written as:

$$R=R_0+R_1\cos2\theta+R_2\cos4\theta, \tag{24}$$

where the R_i are the functions of products $f(\alpha\mathbf{v}_f\leftarrow M_1M_2\mathbf{v}_c)\,f^*(\alpha\mathbf{v}_f\leftarrow M_1'M_2'\mathbf{v}_c)$ of the ionization amplitudes. From (24) one can see that only three parameters can be obtained from the θ-dependence at each velocity $\bar{v}_c$ and therefore not all products of amplitudes ff^* can be determined. As was discussed by Kircz et al. [7] and in more detail by Nienhuis [18, 19] it is not unreasonable to neglect all those products for which $(M_1M_2)\neq(M_1'M_2')$ since they are

likely to yield small contributions to R due to the integration over all directions of $\mathbf{v}_f$ in (23). By doing so one obtains a system of three equations for the coefficients R_0, R_1 and R_2 which depend on cross sections $\sigma(M_1, M_2, \bar{v}_c)$. These equations read:

$$R_0 = N_c/288\left[\left(72+\frac{36}{Q}+\frac{99}{4Q^2}\right)\bar{\sigma}\left(\frac{3}{2}\frac{3}{2}\bar{v}_c\right)+\left(144-\frac{99}{2Q^2}\right)\bar{\sigma}\left(\frac{3}{2}\frac{1}{2}\bar{v}_c\right)+\left(72-\frac{36}{Q}+\frac{99}{4Q^2}\right)\bar{\sigma}\left(\frac{1}{2}\frac{1}{2}\bar{v}_c\right)\right]$$

$$R_1 = N_c/288\left[\left(\frac{108}{Q}+\frac{27}{Q^2}\right)\bar{\sigma}\left(\frac{3}{2}\frac{3}{2}\bar{v}_c\right)-\left(\frac{54}{Q^2}\right)\bar{\sigma}\left(\frac{3}{2}\frac{1}{2}\bar{v}_c\right)+\left(-\frac{108}{Q}+\frac{27}{Q^2}\right)\bar{\sigma}\left(\frac{1}{2}\frac{1}{2}\bar{v}_c\right)\right]$$

$$R_2 = N_c/288\left[\left(\frac{81}{4Q^2}\right)\bar{\sigma}\left(\frac{3}{2}\frac{3}{2}\bar{v}_c\right)-\left(\frac{81}{2Q^2}\right)\bar{\sigma}\left(\frac{3}{2}\frac{1}{2}\bar{v}_c\right)+\left(\frac{81}{4Q^2}\right)\bar{\sigma}\left(\frac{1}{2}\frac{1}{2}\bar{v}_c\right)\right], \tag{25}$$

with the ratio Q given by (22), and:

$$\begin{aligned}
&\bar{\sigma}(\tfrac{3}{2}\tfrac{3}{2}\bar{v}_c) = \tfrac{1}{2}[\sigma(\tfrac{3}{2},\tfrac{3}{2},\bar{v}_c)+\sigma(\tfrac{3}{2},-\tfrac{3}{2},\bar{v}_c)]\\
&\bar{\sigma}(\tfrac{3}{2}\tfrac{1}{2}\bar{v}_c) = \tfrac{1}{2}[\sigma(\tfrac{3}{2},\tfrac{1}{2},\bar{v}_c)+\sigma(\tfrac{3}{2},-\tfrac{1}{2},\bar{v}_c)]\\
&\bar{\sigma}(\tfrac{1}{2}\tfrac{1}{2}\bar{v}_c)+\tfrac{1}{2}[\sigma(\tfrac{1}{2},\tfrac{1}{2},\bar{v}_c)+\sigma(\tfrac{1}{2},-\tfrac{1}{2},\bar{v}_c)].
\end{aligned} \tag{26}$$

Nienhuis [18][2] uses the steady state assumption. From his equations 3.17–3.19, 3.30 and 3.32 one can obtain the "steady state equations" ($Q=-1.5$). The system of (25) can be inverted such that the cross sections are expressed as functions of the R_i. One obtains:

$$\begin{aligned}
\bar{\sigma}\left(\frac{3}{2}\frac{3}{2}\bar{v}_c\right) &= \left(R_0-\frac{1-4Q}{3}R_1-\frac{7+16Q-32Q^2}{9}R_2\right)\Big/N_c\\
\bar{\sigma}\left(\frac{3}{2}\frac{1}{2}\bar{v}_c\right) &= \left(R_0-\frac{1}{3}R_1-\frac{7+32Q^2}{9}R_2\right)\Big/N_c\\
\bar{\sigma}\left(\frac{1}{2}\frac{1}{2}\bar{v}_c\right) &= \left(R_0-\frac{1+4Q}{3}R_1-\frac{7-16Q-32Q^2}{9}R_2\right)\Big/N_c.
\end{aligned} \tag{27}$$

As can be seen in (26), the cross sections $\bar{\sigma}(M_1 M_2 \bar{v}_c)$ indicate mean values of $\sigma(M_1 M_2 \bar{v}_c)$ and $\sigma(M_1 - M_2 \bar{v}_c)$: we cannot distinguish substates with opposite magnetic quantum number $\pm M$ since we use linearly polarized light.

Besides these cross sections $\bar{\sigma}(M_1 M_2 \bar{v}_c)$ we can define a cross section σ_{iso} which is valid for the hypothetical case that the excited atoms are not polarized at all, but form an isotropic ensemble. This cross section is given by:

$$\sigma_{iso} = (R_0 - \tfrac{1}{3}R_1 - \tfrac{7}{9}R_2)/N_c \tag{28}$$

By means of equations (22), (24) and (27) we can now analyse our experimental data, i.e. the θ-dependent ionization signals for different collision velocities $\bar{v}_c$.

So far we have described the collision process in a J-picture, assuming that not only the orbital angular momentum can influence the ionization process. If, on the other hand, the influence of the spin could completely be neglected one could describe the process in an L-picture, resulting in ionization amplitudes $f(M_1 M_2)$ and cross sections $\sigma(M_1 M_2 \bar{v}_c)$ with M_1, M_2 now representing the magnetic quantum numbers of the orbital angular momentum, i.e. $M=0, \pm 1$. The corresponding equations which connect the cross sections σ to the Fourier coefficients R_i, are:

$$\begin{aligned}
&\bar{\sigma}(1\,1\,\bar{v}_c) = [R_0 + Q\cdot R_1 + (2Q^2-1)R_2]/N_c\\
&\bar{\sigma}(1\,0\,\bar{v}_c) = [R_0 - \tfrac{1}{2}(Q+1)R_1 - (1+2Q+4Q^2)R_2]/N_c\\
&\bar{\sigma}(0\,0\,\bar{v}_c) = [R_0 - (1+2Q)R_1 + (1+8Q+8Q^2)R_2]/N_c
\end{aligned} \tag{29}$$

with again,

$$\bar{\sigma}(M_1 M_2 \bar{v}_c) = \tfrac{1}{2}[\sigma(M_1 M_2 \bar{v}_c) + \sigma(M_1 - M_2 \bar{v}_c)] \tag{30}$$

and

$$Q = \frac{\rho_1+\rho_0}{\rho_1-\rho_0} = -\frac{1+B}{B}. \tag{31}$$

Notice that the expressions for $\bar{\sigma}(1\,1\,\bar{v}_c)$ (29) and $\bar{\sigma}(\tfrac{3}{2}\tfrac{3}{2}\bar{v}_c)$ (27) are identical.

4. Results

In Fig. 3 we show the measured ionization signal as a function of the angle θ between the light polarization vector and the collision velocity vector $\mathbf{v}_c$ for four different velocities $\bar{v}_c$. Curves with the functional form (24) have been fitted to the experimental results in order to determine the Fourier coefficients R_i. Measurements have been performed for a large number of velocities and the results for the $\sigma_i = R_i/N_c$ are shown in Fig. 4. (Notice that these "cross sections" can be negative!) We did neither determine absolute densities of excited atoms nor detection effi-

[2] A printing error in equation (3.30) of Nienhuis should be pointed out: the expression for s should be $s=A-C$ instead of $s=A-B$

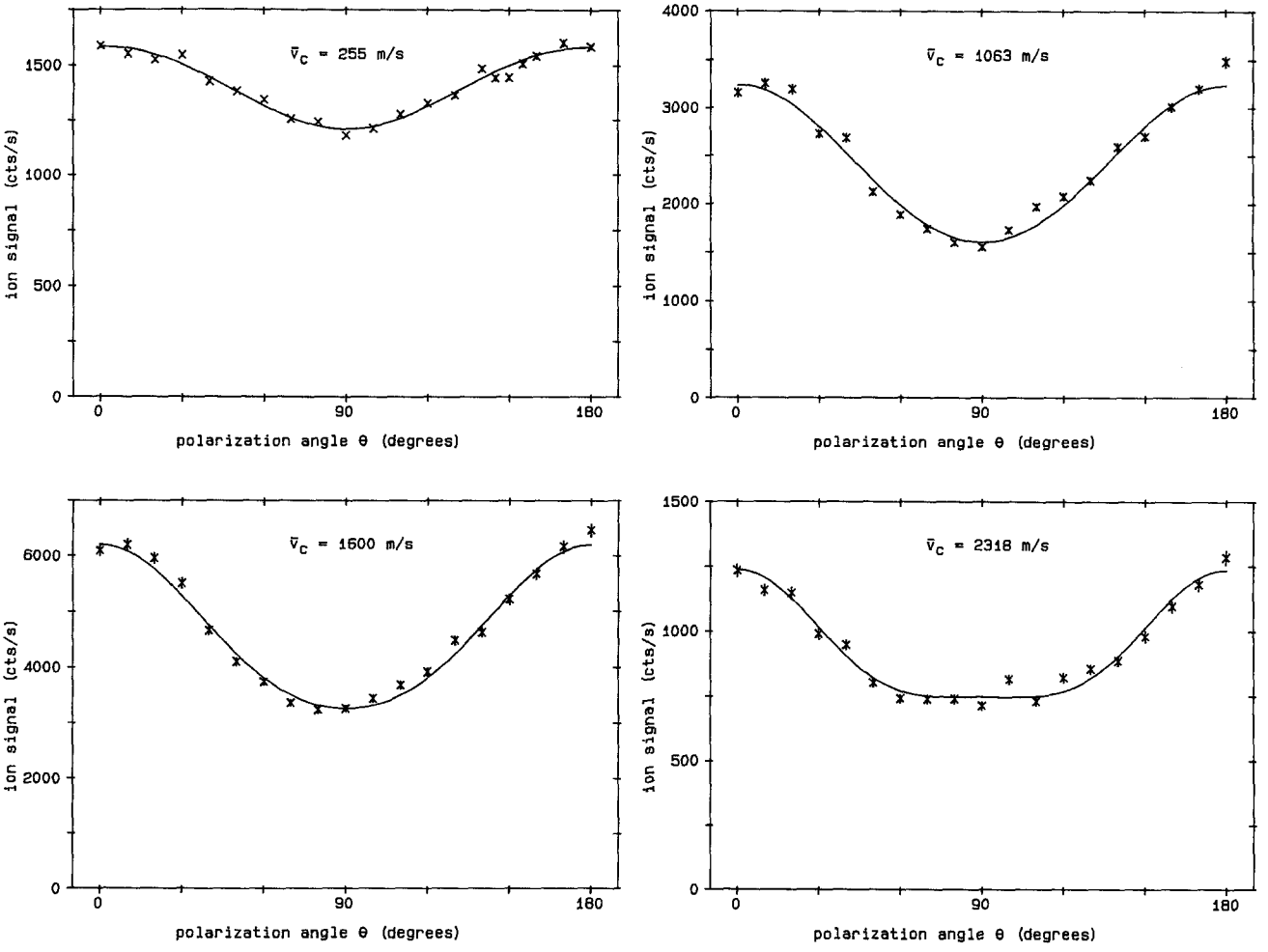

Fig. 3. Ionization signals as a function of the angle θ between the light polarization vector and the collision velocity $\mathbf{v}_c$ for four different velocities $\bar{v}_c$. The ion-signal at $\bar{v}_c = 255$ m/s results from collisions within one beam, whereas the other three result from collisions between atoms from different beams

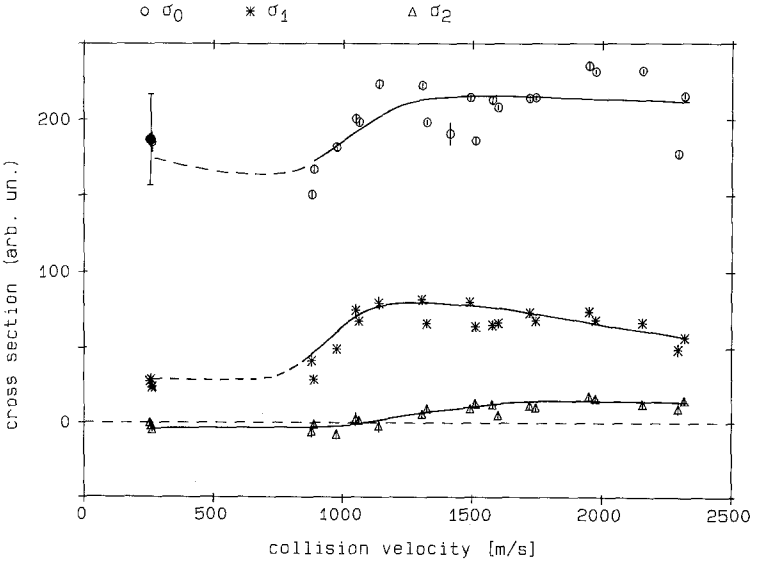

Fig. 4. Results for the cross section σ_0 (the θ-independent part), σ_1 (the $\cos 2\theta$-part) and σ_2 (the $\cos 4\theta$-part) as a function of the relative collision velocity $\bar{v}_c$. The error bars represent only the statistical errors. The points at $\bar{v}_c = 255$ m/s are due to collisions of excited atoms within one beam, and since the interaction volume might be different from that for collisions of atoms from different beams they have a systematic error of 30% in comparison with the other points. This error has been indicated in the σ_0-point

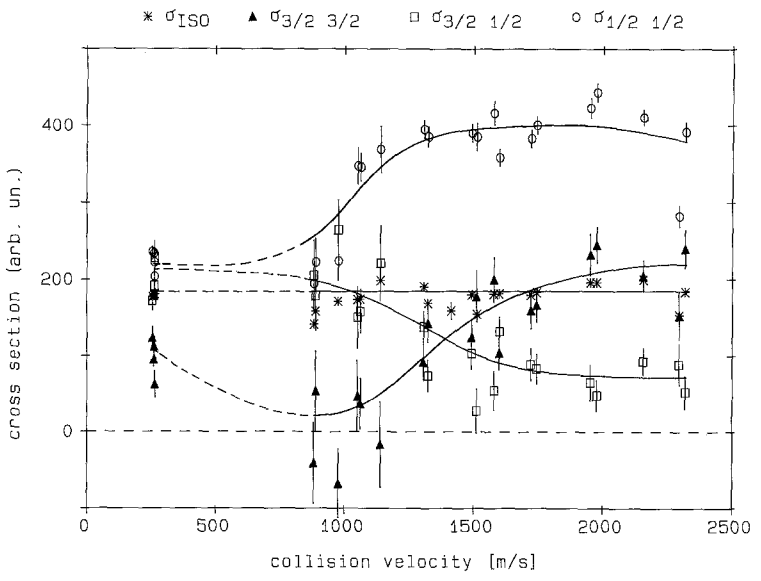

Fig. 5. The cross sections $\bar{\sigma}(1/2, 1/2)$, $\bar{\sigma}(1/2\ 3/2)$, $\bar{\sigma}(3/2\ 3/2)$ and σ_{iso} as a function of $\bar{v}_c$. The units of the y-axis are the same as in Fig. 4. Again the error bars are only statistical errors

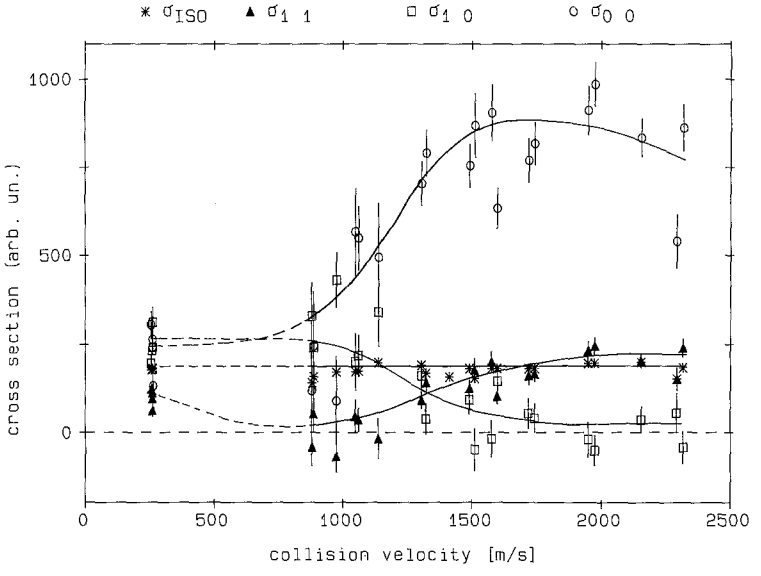

Fig. 6. The cross sections $\bar{\sigma}(00)$, $\bar{\sigma}(10)$, $\bar{\sigma}(11)$ and σ_{iso} as a function of $\bar{v}_c$. The units of the y-axis are the same as in Figs. 4 and 5. Again the errror bars are only statistical errors

ciencies. Therefore we can only give relative values of the σ_i. The error bars in Fig. 4 represent only the statistical errors. The scattering of the σ_i at different velocities appears to be significantly larger than these statistical errors, which means that "long-term errors" (variations in Na densities, Na beam shapes, detection efficiencies) are the more important ones. The results for $\bar{v}_c = 255$ m/s are due to collisions of excited atoms within one atomic beam. Since for these collisions the interaction volume might be different from that for collisions of atoms from different beams, the corresponding σ_i have a systematic error ($\pm 30\%$) with respect to the other values. This error has been indicated in the σ_0-point. From the $\sigma_i(\bar{v}_c)$ we have determined the cross sections $\bar{\sigma}(M_1 M_2 \bar{v}_c)$ and $\sigma_{iso}(\bar{v}_c)$ by means of (22), (27) and (28), respectively. The results are shown in Fig. 5. Again the error bars represent only statistical errors. Finally, Fig. 6 shows the cross sections according to the L-picture description ((29)–(31)).

We did not intend to measure absolute cross sections. Yet we can estimate the cross sections to within a factor of 2–3. We get for σ_{iso}:

$$\sigma_{iso} = 8 \binom{+12}{-5} \cdot 10^{-17}\ \text{cm}^2 \tag{32}$$

Comparison with the result of Huenekens and Gallagher [3], as measured in a vapour cell: $\sigma = 5.1 \cdot 10^{-17}$ cm^2 ($\pm 40\%$), shows very good agreement.

5. Discussion

The velocity dependence of the cross sections $\bar{\sigma}(M_1 M_2 \bar{v}_c)$ allows some conclusions regarding the potential curves involved in the ionization process. However, one always has to keep in mind that the $\bar{\sigma}$ are average cross sections of $\sigma(M_1 M_2\ \bar{v}_c)$ and $\sigma(M_1 - M_2 \bar{v}_c)$ which on their part can be quite different from each other.

As stated in Chapt. 4 neither a description in the J-picture nor one in the L-picture can be excluded. Figures 5 and 6 show that at high velocities a preparation of both atoms in $M_j = \pm\frac{1}{2}(M_L = 0)$ substates is most effective for ionization. The strong increase of the cross section curves above velocities of $\bar{v}_c \sim 900$ m/s indicates that an endothermic process is involved and that a potential barrier with a height of ~ 40 meV has to be overcome in order to reach the ionization continuum. The fact that the cross sections $\bar{\sigma}_J(\frac{1}{2}\frac{1}{2})$ and $\bar{\sigma}_L(0\,0)$ do not vanish at velocities below 900 m/s indicates that in addition ionization via another potential curve takes place which has a lower threshold or which is exothermic.

The cross section $\bar{\sigma}(\frac{3}{2}\frac{1}{2})$ – and the corresponding one $\bar{\sigma}(10)$ in the L-picture – shows an opposite behavior. At velocities above ~ 1000 m/s it decreases significantly. This indicates that ionization takes place at small internuclear distances via an attractive potential curve: at low collision velocities the attraction leads to small distances of closest approach, even for large impact parameters; at higher collision velocities the attraction is less effective and crossing with the continuum at small separations is no longer reached.

Finally, preparation of both atoms in $M_J = \pm 3/2$ states – or both in the $M_L = \pm 1$ state – shows a more complicated behavior of the cross section. It can be explained by assuming that at least two potential curves contribute to ionization: one slightly attractive, with a crossing at very small internuclear distances, and the other repulsive, with a barrier of approximately 60 meV.

So far the discussion is based on the assumption that the preparation of magnetic sublevels with respect to the internuclear axis at infinite distance is conserved throughout the collision, independent of the collision velocity. However rotational coupling could become increasingly important with higher collision velocity and e.g. lead to a significant population of a molecular Σ-state at small separations, when a Δ state is prepared at large internuclear distances. Such an effect could be responsible for the increasing $\bar{\sigma}(\frac{3}{2}\frac{3}{2})$ (or $\bar{\sigma}(11)$) with increasing velocity.

In this situation more quantitative information about diabatic/adiabatic potential curves and coupling matrix elements for the Na*–Na* system is needed. Recently Henriet et al. [20] reported theoretical results which indicate that there is only one adiabatic potential curve crossing into the continuum, it has a $^1\Sigma_u^-$ symmetry and the crossing lies ~ 165 meV above the Na* + Na* separated atom level. The crossing could only be reached at collision velocities above 1800 m/s and there is no experimental evidence that ionization via this crossing is important. More detailed calculations, also of diabatic curves, are being performed [21].

It is worth noting that we observe values for σ_{iso} which do not vary by more than 10% throughout our whole range of velocities.

Finally our assumption should be kept in mind, that the influence of coherence terms can be neglected. This assumption can be checked if the colliding atoms are not preparated identically, but differently. In principle this can be done in our apparatus by changing the polarization properties of the laser light between its intersection with the first and the second atomic beam. Corresponding experiments are just being performed and will be published later. First results indicate a small influence of coherence terms.

Another check on the importance of coherence terms are experiments with circularly polarized light. If coherence terms can be neglected completely the corresponding cross section $\sigma_{circ}(\bar{v}_c)$ can be expressed in terms of the $\bar{\sigma}(M_1 M_2 \bar{v}_c)$, yielding

$$\sigma_{circ} = [18\,\bar{\sigma}(\tfrac{3}{2}\tfrac{3}{2}\,\bar{v}_c) + 108\,\bar{\sigma}(\tfrac{3}{2}\tfrac{1}{2}\,\bar{v}_c) + 16\,\bar{\sigma}(\tfrac{1}{2}\tfrac{1}{2}\,\bar{v}_c)]/288. \quad (33)$$

Preliminary experiments indicate that σ_{circ} is in fact $\sim 30\%$ larger than one would expect from the measured $\sigma(M_1 M_2 \bar{v}_c)$ and (33). The velocity dependence of σ_{circ} however exhibits no significant variation at velocities between $\bar{v}_c = 1000$ m/s and $\bar{v}_c = 2400$ m/s. This is in sharp contrast with results of Wang et al. [11], who also used circularly polarized light and found a sharp decrease by a factor of 5 for σ_{circ} between 1300 and 1500 m/s and a subsequent increase by again a factor of 5 between $\bar{v}_c = 1900$ and 2200 m/s. These discrepancies could not yet be explained. The results of our circularly polarized light measurements will also be presented in a forthcoming publication.

6. Conclusions

We have measured the dependence of associative ionization in Na(3p) + Na(3p) collisions on the polarization and the relative velocity of the collision partners. We have found an increasing polarization dependence for increasing collision velocities. The velocity dependence of cross sections $\bar{\sigma}(M_1 M_2)$ with $M_i = \pm 1/2$ and $\pm 3/2$ was determined. Preparation of both atoms in the $|M_j| = 1/2$ state turned out to yield the highest

ionization at all velocities. All three cross sections show a complex velocity dependence.

We would like to thank G. Nienhuis and H.G.M. Heideman for many stimulating discussions.

References

1. Jong A.A. de, Valk, F. van der: J. Phys. B **12**, L 561 (1979)
2. Kushawa, V.S., Leventhal, J.J.: Phys. Rev. A **22**, 2468 (1980)
3. Huennekens, J., Gallagher, A.: Phys. Rev. A **28**, 1276 (1983)
4. Bonanno, R., Boulmer, J., Weiner, J.: Phys. Rev. A **28**, 604 (1983)
5. Roussel, F., Breger, P., Spiess, G., Manus, C., Geltman, S.: J. Phys. B **13**, L 631 (1980)
6. Carré, B., Spiess, G., Bizau, I.M., Dhet, P., Gérard, P., Wuilleumier, F., Keller, J.C., Le Gouët, J.L., Picqué, J.L., Ederer, D.L., Koch, P.M.: Opt. Commun. **52**, 29 (1984)
7. Kircz, J.G., Morgenstern, R., Nienhuis, G.: Phys. Rev. Lett. **48**, 610 (1982)
8. Rothe, E.W., Theyunni, R., Reck, G.P., Tung, C.C.: Phys. Rev. A **31**, 1362 (1985)
9. Meijer, H.A.J., Meulen, H.P. v.d., Morgenstern, R., Hertel, I.V., Meyer, E., Schmidt, H., Witte, R.: Phys. Rev. A **33**, 1421 (1986)
10. Rothe, E.W., Theyunni, R., Reck, G.P., Tung, C.C.: Phys. Rev. A **33**, 1426 (1986)
11. Wang, M.-X., Vries, M.S. de, Keller, J., Weiner, J.: Phys. Rev. A **32**, 681 (1985)
12. Meijer, H.A.J., Meulen, H.P. v.d., Ditewig, F., Wisman, C.J., Morgenstern, R.: J. Phys. E: Sci. Instrum. **19**, (1987)
13. Hertel, I.V., Schmidt, H., Bähring, A., Meyer, E.: Rep. Prog. Phys. **48**, 375 (1985)
14. Fischer, A., Hertel, I.V.: Z. Phys. A – Atoms and Nuclei **304**, 103 (1982)
15. McClelland, J.J., Kelley, M.H.: Phys. Rev. A **31**, 3704 (1985)
16. Alkemade, C.Th.J.: Spectrochim. Acta **40** B, 1331 (1985)
17. A.R. Edmonds: Drehimpulse in der Quantenmechanik. Mannheim: Bibliographisches Institut 1964
18. Nienhuis, G.: Phys. Rev. A **26**, 3137 (1982)
19. Nienhuis, G.: Polarization effects in associative ionization of excited sodium atoms. In: Electronic and atomic collisions. Lorents, D.C., Meyerhof, W.E., Peterson, J.R. (eds), pp. 569–576. Amsterdam: North-Holland 1986
20. Henriet, A., Masnou-Seeuws, F.: J. Phys. B (in press)
21. Henriet, A.: (Private Communication)

H.A.J. Meijer
H.P. van der Meulen
Fysisch Laboratorium
Rijksuniversiteit Utrecht
Postbus 80.000
NL-3508 TA Utrecht
The Netherlands

R. Morgenstern
Kernfysisch Versneller Instituut
Rijksuniversiteit Groningen
Zernikelaan 25
NL-9747 AA Groningen
The Netherlands

Note Added in Proof

After completion of the manuscript a report was published by Wang et al. (M-X. Wang, J. Keller, J. Boulmer, J. Weiner, Phys. Rev. A **34**, 4497 (1986)) on the same subject. A direct comparison of the results is difficult, since Wang et al. did not deconvolute their measured signal in terms of cross sections for magnetic sublevels. Nevertheless a clear discrepancy between their results and ours can be realized for collision velocities below 750 m/s: their results imply a polarization independent cross section, whereas our measurements exhibit a pronounced dependence (see Fig. 3, and also the results shown in our Ref. 9). The discrepancies could be due to variations in the interaction volumes used by Wang et al. in their different approaches.